Bulletin of the Seismological Society of America. Vol. 66, No. 4, pp. 1343–1373. August 1976

PRELIMINARY EMPIRICAL MODEL FOR SCALING FOURIER AMPLITUDE SPECTRA OF STRONG GROUND ACCELERATION IN TERMS OF EARTHQUAKE MAGNITUDE, SOURCE-TO-STATION DISTANCE, AND RECORDING SITE CONDITIONS

By M. D. Trifunac

ABSTRACT

An empirical model for scaling Fourier Amplitude Spectra of strong earthquake ground acceleration in terms of magnitude, M, epicentral distance, R, and recording site conditions has been presented. The analysis based on this model implies that:

(a) the Fourier amplitude spectra of strong-motion accelerations are characterized by greater energy content and relatively larger amplitudes for long-period waves corresponding to larger magnitudes M,

(b) the shape of Fourier amplitude spectra does not vary appreciably for the distance range between about 10 and 100 km, and

(c) long-period spectral amplitudes ($T > 1$ sec) recorded on alluvium are on the average 2.5 times greater than amplitudes recorded on basement rocks, whereas short-period ($T < 0.2$ sec) spectral amplitudes tend to be larger on basement rocks.

It has been shown that the uncertainties which are associated with the forecasting of Fourier amplitude spectra in terms of magnitude, epicentral distance, site conditions, and component direction are considerable and lead to the range of spectral amplitudes which for an 80 per cent confidence interval exceed one order of magnitude. A model has been presented which empirically approximates the distribution of Fourier spectrum amplitudes and enables one to estimate the spectral shapes which are not exceeded by the presently available data more than 100 $(1-p)$ per cent of time where p represents the desired confidence level ($0 < p < 1$).

Introduction

One of the main practical objectives of the current research work in strong-motion seismology and earthquake engineering is to find the scaling relationships that exist between the amplitudes of strong earthquake ground motion and several parameters which are routinely employed to describe the overall earthquake size and its effect in the near-field. Significant progress has been made during the past 10 years toward better understanding of earthquake mechanisms and the manner in which the properties of earthquake sources influence the amplitudes of recorded motions (e.g., Haskell, 1969; Savage, 1966; Brune, 1970). Numerous detailed studies of several earthquakes (e.g., Mikumo, 1973; Trifunac, 1974; Trifunac and Udwadia, 1974), of the overall trends in body waves (e.g., Thatcher and Hanks, 1973; Hanks and Wyss, 1972; Tucker, 1975), and of surface-wave amplitudes have also been carried out. However, empirical studies of spectral amplitudes in the near-field, which contain all types of waves, were not feasible until this time because the number and the uniformity in the quality of digital processing of recorded accelerograms were inadequate for such investigations. Even now, over 40 years

*Present address: Department of Civil Engineering, University of Southern California, Los Angeles, California 90007.

after the strong-motion recording program in the United States began, the number of recorded accelerograms is far from adequate to provide a sound basis for complete and detailed empirical studies of near-field strong ground motions. Nevertheless, the data which are available offer a basis for a preliminary analysis of spectral amplitudes and can indicate which scaling parameters and what types of empirical models may be suitable for an interim description of strong-motion amplitudes. These data also provide enough information for ongoing research and development in the fields of instrumentation, data collection, and processing techniques, as well as in the search for better and more complete empirical models for use in scaling near-field ground motions.

The purpose of this paper is to present an empirical model for scaling Fourier amplitude spectra in terms of earthquake magnitude, source-to-station distance, and the geological environment of the recording station. Although it is well known (e.g., Brune, 1970; Trifunac, 1973) that the shape of the near-field spectrum cannot be modeled accurately by only one amplitude scaling parameter, such as earthquake magnitude, the difficulties associated with forecasting the stress-drop, the direction, the spatial amplitude distribution and the velocity with which faulting might progress along a postulated fault plane are indeed quite formidable. Therefore, from a practical point of view, it is worthwhile to consider only those parameters which are readily available in routine studies and catalogs of earthquake occurrence. The advantage of such an approach is that, without a detailed and possibly indecisive investigation, one can estimate the expected Fourier spectral amplitudes for a given earthquake magnitude, source-to-station distance and recording-site conditions. The penalty for disregarding other important parameters is then reflected in the scatter of the data about the predicted amplitudes.

Characterization of the amplitudes of strong earthquake ground motion by means of an approximate empirical model, as the one presented in this paper, represents considerable improvement relative to the scaling in terms of peak acceleration, peak velocity, and peak displacement (e.g., Trifunac, 1976). This is because the peaks sample only the spectral amplitudes in a limited frequency band which is centered around the frequency components which build up the peak itself. The scatter of peak amplitudes about the root-mean-square of Fourier spectrum amplitudes, of the representative frequency band, is often considerable, i.e., may have a large standard deviation. Thus, from the peak acceleration alone, for example, it is not possible to make a reliable estimate of the complete Fourier amplitude spectrum. Scaling of spectra by peak acceleration, peak velocity, and peak displacement would be considerably better but would still be characterized by large uncertainties when compared to the direct scaling of the entire spectral amplitudes which is presented in this work.

The analysis presented in this paper is of a preliminary nature and should be interpreted only as an attempt to develop and test a simple approximate model for scaling Fourier amplitude spectra of strong earthquake ground motion in terms of several routinely available parameters. Although considerable thought has been given to the functional form of the model in order that it be capable of incorporating the majority of the important characteristics of recorded accelerograms, it must be emphasized that the model presented here and the method of the analysis will have to be updated and improved as more strong-motion accelerograms become available and as we learn about better empirical models for such analyses.

Available Data

The Fourier amplitude spectra (FS) which are used in this study have been extracted from the Volume III tape (Trifunac and Lee, 1973) which contains absolute acceleration

spectra (SA), relevant displacement spectra (SD), relative velocity spectra (SV), pseudo-relative velocity spectra (PSV) and Fourier amplitude spectra (FS) for 381 strong-motion accelerograms (Hudson *et al.*, 1972a). Of these 381 records, with two horizontal and one vertical component each, 186 accelerograms have been recorded at "free-field" stations or in the basement of tall buildings. For the purpose of this analysis, it has been assumed that these recordings represent strong ground motion which is not seriously affected by the surroundings of the recording station. Detailed investigations will, no doubt, show that the records obtained in the basements of tall buildings or adjacent to some other large man-made or natural structure may be modified by the wave scattering and diffraction caused by these structures. For this analysis, it will be assumed that these variations are averaged out when one considers all records simultaneously, and thus such effects will be neglected.

These 381 accelerograph records resulted from 57 earthquakes in the western United States and were recorded during the period from 1933 to 1971. From the 186 records that could be used as free-field data, only 182 were actually employed in this analysis because no reliable magnitude estimates were available for four records (Table 1). These 182 records were obtained during 46 earthquakes whose published magnitudes (Volume II reports, Parts A through Y, Hudson *et al.*, 1971) range from 3.8 to 7.7. The distribution of this data among five magnitude intervals is as follows: magnitude 3.0 to 3.9, 1 record; 4.0 to 4.9, 5 records; 5.0 to 5.9, 40 records; 6.0 to 6.9, 129 records; and 7.0 to 7.9, 7 records. As may be seen from this distribution, there is a concentration of data between magnitudes 5 and 7 with only 13 records available for magnitudes less than 5.0 and greater than 7.0. A majority (117) of the 182 records were registered at stations which were located on alluvium (classified under $s=0$; see Trifunac and Brady, 1975a for more detailed description of this classification), 52 records were obtained on intermediate type rocks ($s=1$) or close to boundaries between alluvium and basement rocks, and only 13 records came from stations on basement rocks ($s=2$). Of these 182 records more than one half were recorded during the San Fernando, California, earthquake of 1971.

As may be seen from the above paragraph, the data used in this study are far from adequate to describe the complete magnitude range from $M=3$ to $M=8$ and all recording site conditions. There is also a serious shortage of recorded accelerograms on basement rock sites ($s=2$) and for magnitudes greater than $M=7$. Thus, the following analysis is no doubt seriously affected by this shortage and the non-uniformity of data and will have to be repeated and improved when more records become available. Nevertheless, these data do represent the largest collection of uniformly processed accelerograms, so far, and can be used as an interim basis for the preliminary development of empirical models for study of Fourier amplitude spectra.

The Fourier amplitude spectrum of strong motion acceleration can be defined by (e.g., Hudson *et al.*, 1972a)

$$FS(T)\equiv\left|\int_0^S a(t)e^{-i(2\pi/T)t}dt\right|, \tag{1}$$

where T is the period of vibration, $T=2\pi/\omega$, S is the total duration of digitized accelerogram $a(t)$, for $0\leqq t\leqq S$ and $i=\sqrt{-1}$. $FS(T)$ can be shown to correspond to the amplitude of the relative velocity spectrum for an undamped single-degree-of-freedom oscillator at $t=S$ (e.g., Hudson *et al.*, 1972a), and this property of $FS(T)$ can be used to compute the Fourier amplitude spectra simultaneously with the computation of the relative velocity response spectra (Trifunac and Lee, 1973). The Fourier amplitude spectra have also been calculated by using the Fast Fourier Transform technique (FFT) (see Hudson *et al.*, 1972b) and are available in Volume IV reports. In this paper, however, in which we carry out simultaneous regression analysis for all 182 records at 91 selected periods, T, it is preferable to use $FS(T)$ as computed in the Volume III Processing of

TABLE 1

SUMMARY OF ACCELEROGRAMS RECORDED AT "FREE-FIELD" STATIONS OR IN BUILDING BASEMENTS

Earthquake No.*	No. of Accelerograms Used in this Study	Magnitude	Caltech Report No.
1	3	6.3	B021,V314, V315
2	1	5.4	B023
3	—	—	U294
4	1	6.5	B024
5	1	6.0	B025
6	—	—	U295
8	—	—	U297
9	—	—	U298
13	1	5.5	B026
14	1	6.7	A001
15	1	6.4	B027
16	1	5.9	U299
17	1	6.4	U300
18	2	5.4	V316, V317
19	1	6.5	T286
20	1	5.3	U301
21	2	7.1	B028, B029
22	1	5.6	T287
23	1	5.8	A002
24	5	7.7	A003, A004, A005, A006, A007
26	1	5.5	B030
27	1	6.0	V319
28	1	5.5	T288
29	1	5.9	B031
30	1	5.3	U305
31	1	6.3	T289
32	2	6.5	A008, A009
33	1	5.8	A010
36	1	5.4	T292
37	1	6.8	A011
39	1	4.7	V329
40	1	3.8	V320
41	5	5.3	A013, A014, A015, A016, A017
42	2	4.4	V322, V323
43	1	4.0	V328
44	1	5.0	U307
45	1	5.7	U308
46	2	5.7	A018, U309
47	1	5.0	V330
48	2	6.5	B032, U310
49	1	4.0	V331
50	6	5.6	B034, B035, B036, B037, B038, U311
51	1	6.3	T293
52	1	6.3	V332
53	2	5.8	B039, U312
54	1	5.2	U313

TABLE 1—*Continued*

Earthquake No.*	No. of Accelerograms Used in this Study	Magnitude	Caltech Report No.
55	13	6.4	A019, A020, B040, Y370, Y371, Y372, Y373, Y375, Y376, Y377, Y378, Y379, Y380
56	7	5.4	W334, W335, W336, W338, W339, W342, W344
57	98	6.4	C041, C048, C051, C054, D056, D057, D058, D059, D062, D065, D068, E071, E072, E075, E078, E081, E083, F086, F087, F088, F089, F092, F095, F098, F101, F102, F103, F104, F105, G106, G107, G108, G110, G112, G114, H115, H118, H121, H124, I128, I131, I134, I137, J141, J142, J143, J144, J145, J148, K157, L166, L171, M176, M179, M180, M183, M184, N185, N186, N187, N188, N191, N192, N195, N196, N197, O198, O199, O204, O205, O206, O207, O208, O210, P214, P217, P220, P221, P222, P223, P231, Q233, Q236, Q239, Q241, R244, R246, R248, R249, R251, R253, S255, S258, S261, S262, S265, S266, S267

*For further details on these earthquakes see Trifunac and Brady (1975a). Records U296, T274, T275, T276, U302, U303, U304, T290, T291 and A012 which were recorded during the earthquakes numbered 7, 10, 11, 12, 25, 34, 35 and 38 were not included in this analysis. Six of these records represent incomplete time histories. For earthquakes 7 and 25 no reliable magnitude estimates were available.

Response Spectra (Trifunac and Lee, 1973), since these computations have already been carried out at 91 fixed periods for the interval of T from 0.040 to 15 sec. Furthermore, computations in Volume IV which employ the FFT algorithm are based on the discrete time series analysis, while the computations in Volume III are based on the straight-line interpolation between the consecutive points of digitized accelerograms. This straight-line interpolation improves the accuracy of computed Fourier spectrum amplitudes, especially in the high-frequency range close to the Nyquist frequency (Udwadia and Trifunac, 1975). Finally, the FFT algorithm yields Fourier amplitudes at equally spaced frequencies which are multiples of $1/S$. Since S is different for every record, extensive interpolation and smoothing of the computed Fourier spectra would be required before the spectra from the Volume IV tape could be used in the following analysis. For this

reason, $FS(T)$ spectra computed in the Volume III processing were found to be more convenient for use in this study.

All data on the Volume III tape (Trifunac and Lee, 1973) have been presented in terms of seconds for time units and inches for amplitudes, because the Volume III data have been primarily prepared for use in the engineering community. For simplicity, and to preserve a direct relationship with the raw data, we will also employ inches and seconds in this paper, since all amplitudes can easily be multiplied by 2.54 to convert them from inches to centimeters.

Fourier Amplitude Spectra of Digitization Noise

Before proceeding with the regression analysis of Fourier amplitude spectra, it is necessary to examine the extent to which the computed Fourier spectra are affected by digitization and processing noise in the frequency band of interest which is between 0.07 Hz (or 0.125 Hz) and 25 Hz. Routine data processing techniques (Trifunac and Lee, 1973) which have been designed for typical accelerograms simply band-pass filter raw digitized data between 0.07 and 25 Hz or between 0.125 and 25 Hz depending on whether the raw data have been digitized from paper or 70- and 35-mm film records. However, since the digitization noise does not have constant spectral amplitudes in the respective frequency bands and since these amplitudes depend on the total length of record which has been digitized, for the analysis in this paper it is necessary to extend the results presented by Trifunac *et al.* (1973a) and compute the average Fourier amplitude spectra of digitization noise for different record durations.

Six operators digitized a straight line twice and one operator digitized it once, thus producing a total of 13 digitizations. The straight line which they digitized extended diagonally from the lower left corner to the upper right corner of a rectangular Mylar transparency, 10 in high and about 23 in long. The total average number of digitized points had been selected to be about 700, which corresponds to about 30 pts/inch. This digitization rate was chosen to correspond to the average digitization rate for 4× enlargements of 10- to 15-cm-long segments of 70-mm film records from which an average operator would digitize about 40 to 50 points per 4 cm which corresponds to a time interval of 1 sec. The reasons for selecting a sloping straight line to analyze digitization noise and other pertinent details of this and related procedures have been discussed by Trifunac *et al.* (1973a) and will not be repeated here.

To simulate the effect of fixed base line with respect to which all accelerograms are routinely digitized in order to eliminate long-period distortions, we decimated all raw digitizations of the straight line and kept only 16 points from the total sequence of about 700 points. For the 4× enlargements of 70-mm film records, this corresponds to digitization of the fixed base line at equal intervals of about 1 sec long. By smoothing these decimated data with a $\frac{1}{4}, \frac{1}{2}, \frac{1}{4}$ filter and by subtracting the result from the raw digitization, the long-period drifts were thus eliminated from the raw data by following the same procedures used in routine processing of recorded accelerograms which contain fixed mirror traces. An example of a typical acceleration noise for a 15-sec-long record after it has been processed through the routine Volume II (Trifunac and Lee, 1973) band-pass filtering is shown in Figure 1. Once- and twice-integrated acceleration noise data are also shown in this figure to illustrate what may be the typical appearance of velocity and displacement curves which result from the digitization noise. Table 2 presents the average and standard deviations for the peaks of acceleration, velocity and displacement computed from 13 records for the duration of noise records equal to 15, 30, 60 and 100 sec. The peak displacement amplitudes in this table are smaller by a factor of 2 to 3 than the

estimates of the overall accuracy of computed ground displacements by Trifunac and Lee (1974). This could be explained as follows. First, the typical 70-mm record, which is longer than about 15 sec, is digitized in segments which are about 10 to 15 sec long. Moving the record to digitize successive segments adds a "saw-tooth-like" sequence of straight lines to the digitized amplitudes and, thus, additional long-period errors which are not present in

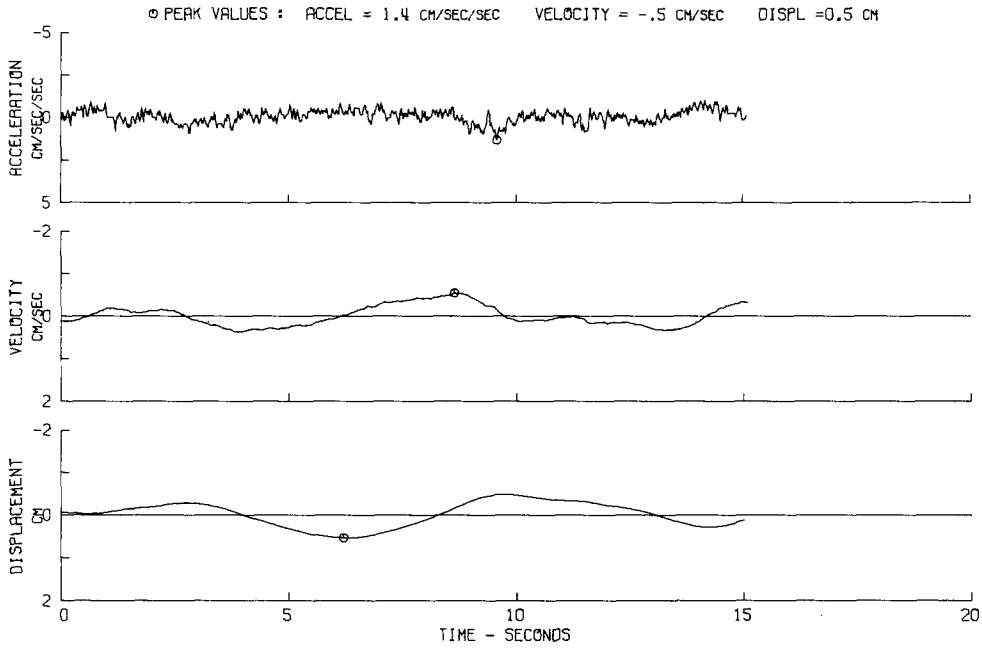

FIG. 1. Typical contributions to acceleration, velocity, and displacement records for instrument and baseline corrected data that result from digitization noise.

TABLE 2

AVERAGES AND STANDARD DEVIATION OF PEAK ACCELERATION, PEAK VELOCITY, AND PEAK DISPLACEMENT THAT MAY BE EXPECTED TO RESULT FROM DIGITIZATION NOISE ALONE

		Duration of Noise Record			
		15 sec	30 sec	60 sec	100 sec
acceleration	ave.	1.66	1.72	1.75	1.74
(cm/sec^2)	st. dev.	0.48	0.48	0.46	0.46
velocity	ave.	0.46	0.55	0.59	0.58
(cm/sec)	st. dev.	0.13	0.15	0.14	0.13
displacement	ave.	0.49	0.61	0.68	0.73
(cm)	st. dev.	0.19	0.18	0.19	0.19

the 13 noise digitizations studied in this paper. The long-period noise contributions resulting from this "saw-tooth-like" error are eliminated from the digitized data off 70-mm film records which have all been high-pass filtered from 0.125 Hz rather than from 0.07 Hz (see Trifunac *et al.*, 1973b), but some intermediate frequency errors are still present in the data. Second, and probably a more important reason for peak displacements in Table 1

being two to three times smaller than our previous estimates of the overall displacement errors (Trifunac and Lee, 1974), is that this noise study was carried out under more uniform and controlled conditions than the actual digitizations of the 381 accelerograph records, which took several years to complete and involved many more operators and different digitizing equipment as well.

For the purpose of this and other related investigations we will assume that the characteristics of the above described "noise" accelerograms are satisfactory to describe approximately the overall noise amplitudes in 182 records for short and intermediate periods, T, and we will use the average Fourier amplitude spectra of these 13 digitizations to carry out an approximate scheme of noise subtraction from the computed Fourier amplitude spectra of 546 accelerograms. The amplitudes of the average and of the average plus one standard deviation of spectral amplitudes of noise are shown in Figures 3 through 6.

Empirical Model for Scaling Fourier Amplitude Spectra

In a recent study Trifunac (1976) presented an approximate model for estimating the range of possible peak amplitudes of strong ground motion for known earthquake magnitude, source-to-station distance and recording-site conditions. The same empirical model can be applied to scaling of spectral amplitudes at a selected set of discrete periods, T. For this purpose equation (4) from our previous work (Trifunac, 1976) can be generalized to become

$$\log_{10}[FS(T)_{,p}] = M + \log_{10} A_0(R) - \log_{10}\{FS_0(T, M, p, s, v, R)\} \tag{2}$$

where M is earthquake magnitude, p is the confidence level selected for the approximate bound of spectral amplitudes $FS(T)_{,p}$, s represents the type of site conditions ($s=0$ for alluvium, $s=1$ for intermediate rocks, and $s=2$ for basement rocks), v designates the horizontal or vertical components ($v=0$ for horizontal, $v=1$ for vertical) and $\log_{10} A_0(R)$ represents an empirical function (Richter, 1958) which describes the amplitude attenuation with distance. $FS_0(T, M, p, s, v, R)$ represents another empirical scaling function for which we hypothesize the form

$$\log_{10} FS_0(T, M, p, s, v, R) = a(T)p + b(T)M + c(T) + d(T)s + e(T)v + f(T)M^2 + g(T)R, \tag{3}$$

where $a(T), b(T), \ldots, f(T)$ and $g(T)$ are as yet unknown functions of T which will be determined in the following regression analysis. In this paper, as in the analysis of peak amplitudes (Trifunac, 1976), the higher order terms in p, s and M and the terms which include different products of p, s and M will be neglected.

Equation (3) introduces a new term $g(T)R$ the analog of which was not present in our previous study (Trifunac, 1976). This term now models the period-dependent attenuation correction factor for distance R and its form corresponds to the usual amplitude attenuation $\exp(-\pi R/Q\beta T)$, on a linear scale, which is often employed to model approximately the effects of anelastic attenuation. Here β stands for the shear-wave velocity and Q is the attenuation constant. In (3) $g(T)$ then might be thought of as corresponding to $\pi/Q\beta T \log_{10} e$.

If the $\log_{10} A_0(R)$ term were to represent the geometric spreading only, the $g(T)R$ would model the equivalent anelastic attenuation. However, $\log_{10} A_0(R)$, which has been derived empirically from the data on actual peak amplitudes in Southern California, represents an average combination of geometric spreading and anelastic attenuation for a

frequency band centered around 1 Hz. Therefore, the term $g(T)R$ cannot be thought of as modeling $\pi/Q\beta T \log_{10} e$ but rather represents a correction to the average attenuation which is represented by $\log_{10} A_0(R)$. In the study of peak accelerations, peak velocities and peak displacements (Trifunac, 1976), a term like $g(T)R$ was omitted on purpose to avoid undue emphasis and dependence in the model on the digitization noise which is reflected in larger peak amplitudes, especially for displacements, at distances which are typically greater than 100 km. In this paper, because Fourier amplitude spectra are being studied, it is possible to subtract the expected contributions to spectral amplitudes that result from noise; the $g(T)R$ then reflects actual corrections to the $\log_{10} A_0(R)$ term.

Regression Analysis

The computation of the coefficient functions $a(T), b(T), \ldots, f(T)$ and $g(T)$ in equation (3) was carried out at 91 discrete periods T ranging from 0.04 to 15.0 sec. From each of the 546 Fourier amplitude spectra an average noise spectrum was first subtracted. This noise spectrum was obtained by linearly interpolating from the spectra which were computed for 15, 30, 60 and 100 sec (Figures 3 through 6) to obtain a noise spectrum which would apply for a record with the actual duration (Table 3) of each accelerogram. The data for $\log_{10}\{FS_0(T, M, p, s, v, R)\}$ in equation (2) were then computed by subtracting from $\log_{10}[FS(T)]$ the respective magnitude and $\log_{10} A_0(R)$ for the epicentral distance R corresponding to each of 182 records. Regression analysis was then carried out for each of 91 periods by fitting the right-hand side of equation (3) to the data for $\log_{10}\{FS(T, M, p, s, v, R)\}$.

To carry out regression analysis on $\log_{10}\{FS_0(T, M, p, s, v, R)\}$ with $a(T), b(T), \ldots, f(T)$ and $g(T)$ as coefficients at a fixed value of T, we began by partitioning all data into five groups corresponding to magnitude groups 3.0–3.9, 4.0–4.9, 5.0–5.9, 6.0–6.9 and 7.0–7.9. The data in each of these groups were next grouped according to the site classifications $s=0$, $s=1$ and $s=2$. The data within each of these subgroups were then divided into two parts corresponding to $v=0$ and $v=1$. The n data remaining in each of these final parts were next rearranged so that the numerical values of $\log_{10}\{FS_0(T, M, p, s, v, R)\}_i$ for $i=1, 2, 3, \ldots, n$ decrease monotonically with increasing i. Then, if $m=$integer part of (pn), the mth data point represents an estimate of $\log_{10}\{FS_0(T, M, p, s, v, R)\}$ which is to be associated with the p-percent confidence level. If the number of data points, n, in each group was greater than 19, we used 19 levels for subsequent least-squares fitting with the p levels equal to 0.5, 0.10, 0.15, ..., 0.9 and 0.95. If the number of data points in each group was less than 19, we used all data points and computed the estimates of the corresponding confidence levels p from the fraction of points that were smaller than a given level to the total number of points in that group of n. This approximate scheme has the effect of decreasing the "weight" of data groups for which many points are available in the subsequent least-squares fitting.

For those accelerograms which were high-pass filtered from 0.125 Hz rather than from 0.07 Hz (Table 3) the data on $\log_{10}\{FS_0(T, M, p, s, v, R)\}$ have not been included in the regression analysis for periods, T, longer than 8 sec. This and the fact that for many intermediate and small earthquakes spectral amplitudes for the long-period waves have a small signal-to-noise ratio led to the decision to terminate the final computation and presentation of $a(T), b(T), \ldots, f(T)$ and $g(T)$ at the long-period end equal to 12 sec rather than at 15 sec.

Figure 2 presents the results of least-squares fitting of equation (3) to $\log_{10}\{FS_0(T, M, p, s, v, R)\}$ data. The discrete estimates of $a(T), b(T), \ldots, f(T)$ and $g(T)$ have been connected with straight lines to illustrate the degree of variability and "noise"

TABLE 3

TOTAL DURATION AND LOW CUTOFF FREQUENCY FOR ACCELERATION RECORDS USED IN THIS STUDY

Record No.	Caltech Report No.	Total Duration*	Low-Frequency Cutoff (Hz)
1	A001	54	0.07
2	A002	56	0.07
3	A003	77	0.07
4	A004	54	0.07
5	A005	75	0.07
6	A006	83	0.07
7	A007	79	0.07
8	A008	78	0.07
9	A009	42	0.07
10	A010	51	0.07
11	A011	90	0.07
12	A013	25	0.07
13	A014	26	0.07
14	A015	27	0.07
15	A016	25	0.07
16	A017	40	0.07
17	A018	40	0.07
18	A019	87	0.07
19	A020	79	0.07
20	B021	99	0.07
21	B023	75	0.07
22	B024	90	0.07
23	B025	51	0.07
24	B026	71	0.07
25	B027	67	0.07
26	B028	67	0.07
27	B029	89	0.07
28	B030	58	0.07
29	B031	65	0.07
30	B032	82	0.07
31	B034	44	0.07
32	B035	26	0.07
33	B036	44	0.07
34	B037	30	0.07
35	B038	30	0.07
36	B039	30	0.07
37	B040	45	0.07
38	C041	31	0.07
39	C048	59	0.07
40	C051	52	0.07
41	C054	57	0.07
42	D056	62	0.07
43	D057	82	0.07
44	D058	79	0.07
45	D059	57	0.07
46	D062	54	0.07
47	D065	41	0.07
48	D068	37	0.07
49	E071	30	0.07
50	E072	54	0.07
51	E075	44	0.07
52	E078	57	0.07

TABLE 3—*Continued*

Record No.	Caltech Report No.	Total Duration*	Low-Frequency Cutoff (Hz)
53	E081	50	0.07
54	E083	63	0.07
55	F086	78	0.07
56	F087	81	0.07
57	F088	30	0.07
58	F089	59	0.07
59	F092	34	0.07
60	F095	67	0.07
61	F098	56	0.07
62	F101	11	0.07
63	F102	10	0.07
64	F103	27	0.07
65	F104	11	0.07
66	F105	64	0.07
67	G106	31	0.125
68	G107	29	0.125
69	G108	99	0.125
70	G110	98	0.125
71	G112	52	0.125
72	G114	58	0.125
73	H115	40	0.125
74	H118	86	0.125
75	H121	46	0.125
76	H124	33	0.125
77	I128	27	0.125
78	I131	48	0.125
79	I134	49	0.125
80	I137	57	0.125
81	J141	60	0.07
82	J142	37	0.125
83	J143	35	0.07
84	J144	37	0.07
85	J145	99	0.125
86	J148	19	0.125
87	K157	32	0.125
88	L166	65	0.125
89	L171	53	0.07
90	M176	88	0.125
91	M179	13	0.07
92	M180	99	0.125
93	M183	20	0.125
94	M184	30	0.125
95	N185	44	0.125
96	N186	59	0.125
97	N187	30	0.125
98	N188	45	0.125
99	N191	70	0.125
100	N192	25	0.125
101	N195	99	0.125
102	N196	53	0.125
103	N197	43	0.125
104	O198	31	0.125
105	O199	35	0.125
106	O204	69	0.07

Continued

TABLE 3—*Continued*

Record No.	Caltech Report No.	Total Duration*	Low-Frequqncy Cutoff (Hz)
107	O205	99	0.07
108	O206	53	0.125
109	O207	62	0.07
110	O208	62	0.125
111	O210	54	0.125
112	P214	30	0.07
113	P217	30	0.07
114	P220	61	0.07
115	P221	30	0.07
116	P222	58	0.07
117	P223	33	0.07
118	P231	48	0.125
119	Q233	37	0.125
120	Q236	42	0.125
121	Q239	45	0.125
122	Q241	49	0.125
123	R244	42	0.125
124	R246	44	0.125
125	R248	45	0.125
126	R249	41	0.125
127	R251	31	0.125
128	R253	36	0.125
129	S255	30	0.125
130	S258	48	0.125
131	S261	39	0.125
132	S262	36	0.125
133	S265	21	0.125
134	S266	35	0.125
135	S267	49	0.125
136	T286	71	0.07
137	T287	60	0.07
138	T288	86	0.07
139	T289	78	0.07
140	T292	43	0.07
141	T293	75	0.07
142	U294†	59	0.07
143	U295†	21	0.07
144	U297†	9	0.07
145	U298†	76	0.07
146	U299	62	0.07
147	U300	68	0.07
148	U301	56	0.07
149	U305	57	0.07
150	U307	77	0.07
151	U308	82	0.07
152	U309	88	0.07
153	U310	74	0.07
154	U311	72	0.07
155	U312	93	0.07
156	U313	61	0.07
157	V314	99	0.07
158	V315	99	0.07
159	V316	67	0.07
160	V317	62	0.07

TABLE 3—*Continued*

Record No.	Caltech Report No.	Total Duration*	Low-Frequency Cutoff (Hz)
161	V319	49	0.07
162	V320	36	0.07
163	V322	49	0.07
164	V323	23	0.07
165	V328	26	0.07
166	V329	69	0.07
167	V330	75	0.07
168	V331	7	0.07
169	V332	43	0.07
170	W334	17	0.07
171	W335	38	0.07
172	W336	10	0.07
173	W338	30	0.07
174	W339	42	0.07
175	W342	23	0.07
176	W344	23	0.07
177	Y370	85	0.07
178	Y371	82	0.07
179	Y372	52	0.07
180	Y373	42	0.07
181	Y375	54	0.07
182	Y376	60	0.07
183	Y377	44	0.07
184	Y378	21	0.07
185	Y379	62	0.07
186	Y380	51	0.07

*Rounded to nearest second.

†Not included in the analysis because of incomplete information on earthquake magnitude.

that are associated with each of these functions. The smoothed $a(T), b(T), \ldots, f(T)$ and $g(T)$ have been computed by low-pass filtering the data with an Ormsby filter along the $\log_{10} T$ axis and are also shown in Figure 2.

For fixed T, p, s, v and R, $\log_{10}\{FS_0(T, M, p, s, v, R)\}$ represents a parabola when plotted versus M. The particular choice of a parabola in equation (3) has no physical significance and has been motivated by our previous work which dealt with peaks of strong ground motion (Trifunac, 1976), by the simplicity of its functional form and by the observation that the local amplitudes of near-field strong ground motion, for the limited range of periods considered in that analysis ($T < 15$ sec), seem to cease to grow appreciably with an increase in M for large earthquakes (Trifunac, 1973). Thus, by employing the approximate model which is defined by equation (2), and after the coefficients $a(T), b(T), \ldots, f(T)$ and $g(T)$ have been determined by regression, we assume that $\log_{10}\{FS(T)_{,p}\}$ grows linearly with M up to some magnitude $M_{\min}$. Between $M_{\min}$ and $M_{\max}$ $\log_{10}\{FS(T)_{,p}\}$ still grows with M but with a slope which is less than 1 until the maximum is reached at $M_{\max}$. For magnitudes greater than $M_{\max}$, we assume that the amplitude of $\log_{10}\{FS(T)_{,p}\}$ remains constant and equal to its value for $M = M_{\max}$. Since the functional form of the growth of $\log_{10}\{FS(T)_{,p}\}$ is not known at this time and cannot be determined empirically from the limited number of available data points, we approximate it, quite arbitrarily, by a

parabola between M_{min} and M_{max}. With these restrictions equation (3) becomes $\log_{10}\{FS_0(T, M, p, s, v, R)\} =$

$$a(T)p+b(T)M+c(T)+d(T)s+e(T)v+f(T)M^2-f(T)(M-M_{max})^2+g(T)R \quad \text{for } M \geqq M_{max}$$

$$a(T)p+b(T)M+c(T)+d(T)s+e(T)v+f(T)M^2+g(T)R \quad \text{for } M_{min} \leqq M \leqq M_{max}$$

$$a(T)p+b(T)M_{min}+c(T)+d(T)s+e(T)v+f(T)M_{min}^2+g(T)R \quad \text{for } M \leqq M_{min}. \tag{4}$$

Table 4 presents the values and definitions of M_{min} and M_{max} for six selected periods which range from 0.05 to 10.0 sec. As may be seen from this table, this analysis suggests that $\log_{10}\{FS(T)_p\}$ may cease to grow linearly with M for earthquakes between $M=4$ and $M=5.5$ and that it perhaps reaches its maxima for magnitudes ranging from about $M=7.5$ to about $M=8.5$ and higher. These estimates of M_{min} and M_{max} are more reliable for periods, T, which are not close to the left and right limits of the T interval considered in this

TABLE 4

MAGNITUDE INTERVAL $M_{min} \leqq M \leqq M_{max}$ IN WHICH EQUATION (3) APPLIES

Period T–sec	M_{min}*	M_{max}†
0.05	4.3	7.8
0.10	4.7	7.7
0.50	4.3	8.6
1.00	4.8	8.6
5.00	5.3	7.8
10.00	4.1	9.1

*$M_{min} = -[b(T)/2f(T)]$, see equation (3).
†$M_{max} = [1 - b(T)/2f(T)]$, see equation (3).

study, because M_{min} and M_{max} depend on smoothed amplitudes of $b(T)$ and $f(T)$ which tend to be distorted in the vicinity of the left and right ends by the process of digital filtering. The range of estimates for M_{min} and M_{max} can, of course, only be taken as tentative, since there is not an adequate number of recordings for M greater than 7 and less than 5.

The range of values for M_{min} and M_{max} in Table 4 is in fair agreement with similar estimates of M_{min} and M_{max} in the related analysis of the dependence of peak acceleration, peak velocity and peak displacement on magnitude (Trifunac, 1976). This agreement, however, only shows that there is consistency of interpretation between these two similar models in the study of different characteristics of the same data, but it does not provide an independent support for the choice of these models or for the analysis which is based on these models. We are presenting the estimates of M_{min} and M_{max} in this paper and discussing their possible physical meaning as it may relate to our present understanding of the earthquake source mechanism to show that the regression analysis in this paper does not lead to unreasonable inferences when applied outside the range for which the data are now available. The final test, as well as the improvement of the model, can only come from numerous recordings of representative strong-motion records in the future.

The confidence level function $a(T)$ first increases from about -1.7 for short periods to about -1.4 at periods of about 0.3 sec and then decreases to about -1.8 at the long-period end. This means that the spread of spectral amplitudes about the mean level is smallest close to the period equal to 0.3 sec and that it grows for shorter and longer periods to reach its maximum at the two extreme ends of the T interval. The numerical values of $a(T)$ are about 1.5 to 2 times greater than the corresponding coefficients in similar correlations of peak acceleration ($a \approx -0.9$), peak velocity ($a \approx -1.1$), and peak displacement ($a \approx -1.3$) (Trifunac, 1976). This is as one might expect, since the peak of a time function scales proportional the root-mean-square value of its Fourier amplitude spectrum (Udwadia and Trifunac, 1974). This tends to smooth out the amplitude variations, while $a(T)$ represents the spread of raw unsmoothed Fourier amplitude spectra.

The amplitudes of the site-dependent function $d(T)$ are negative for periods shorter than about 0.2 sec. This means that the spectral amplitudes are, on the linear scale, up to about 1.5 times greater at basement rock sites ($s=2$) than on alluvium ($s=0$). For periods greater than 0.2 sec $d(T)$ becomes positive and reaches a nearly constant level equal to about 0.2 for periods greater than 1.0 sec. For these long periods equation (2) indicates that the spectral amplitudes recorded on alluvium ($s=0$) are on the average about 2.5 times greater than the average spectral amplitudes recorded on basement rock sites ($s=2$). It is interesting to observe that the corresponding d coefficient for peak displacements (Trifunac, 1976) is 0.2 as well.

Gutenberg and Richter (1956) in their studies of the effects of site conditions on the average peak amplitudes also found a factor of 0.4 difference on the logarithmic scale between the sites located on alluvium and the sites on basement rocks. Their inference is in excellent agreement with the results of this analysis for periods longer than about $\frac{3}{4}$ to 1 sec. Furthermore, more detailed perusal of Figure 8 in Gutenberg's (1957) paper, for example, shows that the general trend of the observed ratios of peak amplitudes versus period recorded on alluvium (in Pasadena) to the amplitudes recorded on basement rock (in the Seismological Laboratory) follows the same general trend as that indicated by $d(T)$ in Figure 2. Thus, a detailed study of Gutenberg's (1957) paper shows that the nature of $d(T)$ for periods longer than about 0.2 sec has been available in the literature for almost 20 years. It was necessary, however, to collect accurate high-frequency information by recording with strong-motion accelerographs before it became possible to extend this information about $d(T)$ toward periods shorter than 0.2 sec.

In the high-frequency range $d(T)$ changes sign from negative to positive at 0.2-sec period. If it is assumed that the corresponding coefficient d in the regression analysis for peak acceleration could be approximated by averaging $d(T)$ over the high-frequency band from say 0.04 to 0.5 sec, then the coefficient d would be very close to zero. This is indeed the case, since we found d to be 0.06 (Trifunac, 1976). This confirms the observation that peak accelerations are not very sensitive to site conditions.

Function $e(T)$ in Figure 2 shows that for frequencies greater than about 10 Hz, Fourier amplitude spectra of vertical acceleration are greater than those for horizontal accelerations. For periods longer than 0.1-sec, horizontal amplitudes of Fourier Spectra are considerably larger than the amplitudes of spectra for vertical accelerations. Furthermore, the amplitudes of $e(T)$ for periods longer than about 0.2 sec are fairly consistent with similar estimates of coefficient e for peak accelerations ($e \approx 0.33$), peak velocity ($e \approx 0.34$), and peak displacement ($e \approx 0.24$) (Trifunac, 1976).

The amplitudes of $g(T)$ are small and vary from -0.0005 to about -0.0015 throughout the period range from 0.04 to 12 sec (Figure 2). This means that for a typical distance, say $R = 100$ km, the correction term $g(T)R$ in equation (3) contributes at most 0.15 on the logarithmic scale, i.e., by a factor of 1.4 on the linear amplitude scale. Considering the

spread of spectral amplitudes for a fixed set of parameters and the values of $a(T)$, it appears that $g(T)R$ represents only a minor correction to the overall average scaling of amplitudes versus distance in terms of the $\log_{10} A_0(R)$ function. This means that $\log_{10} A_0(R)+R/1000$ would represent a good approximation for scaling Fourier spectral amplitudes for all periods between 0.04 and 12 sec.

Characteristics of the Model

Figures 3 and 4 show the Fourier amplitude spectra for horizontal and vertical ground motion at $R=0$, for magnitudes $M=4.5$, 5.5, 6.5 and 7.5, and for a 50 per cent confidence level ($p=0.50$). The average and the average plus one standard deviation of the smoothed spectra that would result from digitization noise are also shown.

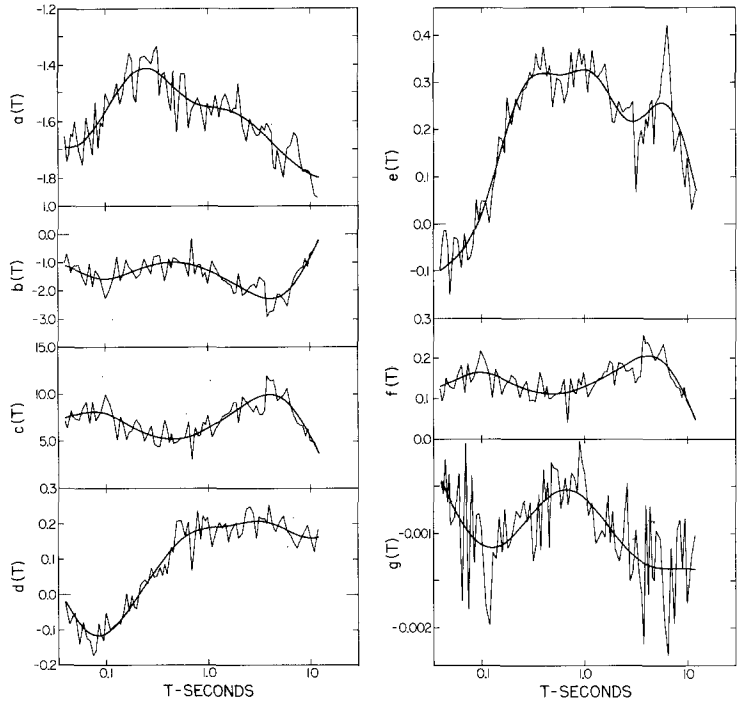

FIG. 2. Scaling functions $a(T), b(T), \ldots, f(T)$ and $g(T)$.

Formally, equation (2) implies that the spectra $FS(T)$ computed at $R=0$ represent the maximum spectral amplitudes for all other parameters held constant. Since an adequate number of Fourier amplitude spectra computed from recorded strong-motion accelerograms is available only for a distance range between about 20 and 250 km and because the $\log_{10} A_0(R)$ curve may not be the best representation for the amplitude variation with distance for R less than about 10 to 20 km for all magnitudes (e.g., see Trifunac, 1976), the spectra in Figures 3 and 4 only represent extrapolations based on equation (2) and at this time cannot be tested by the recorded strong-motion data. However, because the $g(T)R$ term contributes a negligible amount to spectral amplitudes at distances less than 20 km, the shape of the Fourier spectra at say $R=20$ km and at $R=0$ km is very similar. Because in the following discussion we intend to examine some spectral characteristics at $R=0$ km, which are based on the properties of shallow and surface earthquake sources, for consistency we chose to present the spectra in Figures 3 and 4 for epicentral distance $R=0$.

In the near-field of strong earthquake ground motion, permanent displacements which are caused by relative motions on shallow and surface faults represent important contributions to the total displacement history. For ground motions associated with very long wavelengths (long periods, T) permanent displacements contribute virtually all significant spectral amplitudes. As $T \to \infty$, the Fourier amplitude spectrum of ground displacements in the near-field or at the fault itself tends to $uT/2\pi$ (Trifunac, 1973), where u

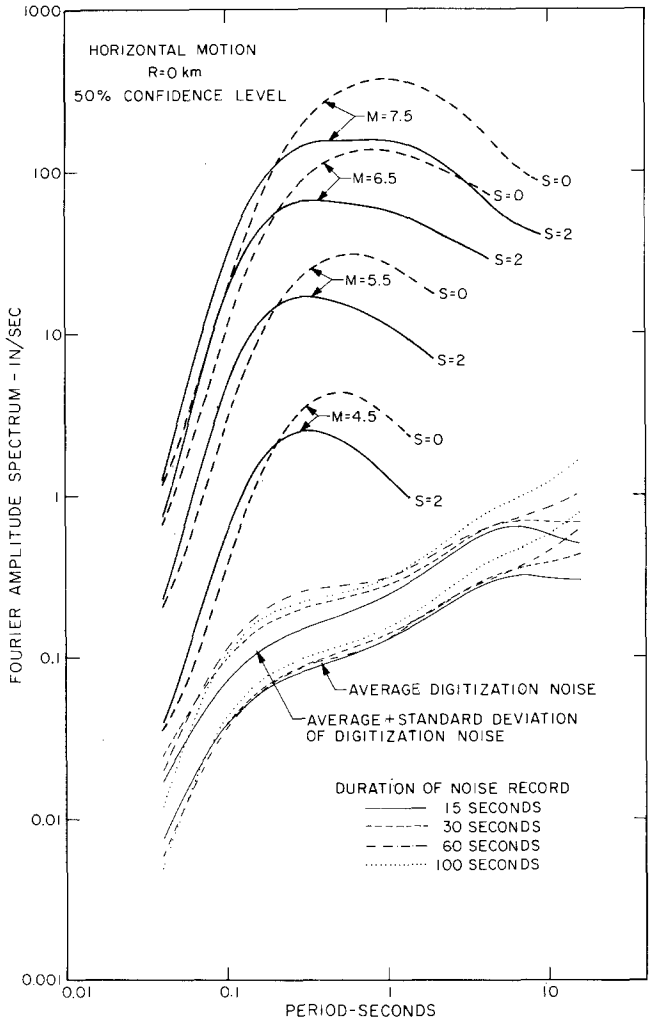

FIG. 3. Horizontal Fourier amplitude spectra of strong-motion acceleration for $R=0$, $p=0.50$, $s=0$ and 2 and for magnitudes equal to 4.5, 5.5, 6.5, and 7.5.

represents the permanent static displacement after the earthquake. The Fourier amplitude spectrum of long-period accelerations would then tend to $2\pi u/T$. This implies that on the log-log plot the $FS(T)$ should have a slope of -1 as $T \to \infty$ at $R=0$. Figures 3 and 4 suggest that this condition may be satisfied for periods longer than about 0.5 sec for magnitude $M=4.5$ earthquakes and for periods longer than about 3 sec for magnitude 7.5 earthquakes. This statement is, of course, applicable only to the average spectral trends ($p=0.5$) as those shown in Figures 3 and 4. The spectra of individual earthquakes may deviate from this average trend considerably because of radiation patterns, interference

created by the moving dislocation, relative position of the recording station and numerous other factors which cannot be considered explicitly in this simplified analysis. How large these deviations may be is illustrated by the amplitude of $a(T)$ in Figure 2.

The expected value of the Fourier spectrum amplitudes computed from digitization noise (Figures 3, . . ., 5 and 6) had been subtracted from the Fourier amplitude spectra of the digitized accelerograms before the regression analysis was carried out. However, this

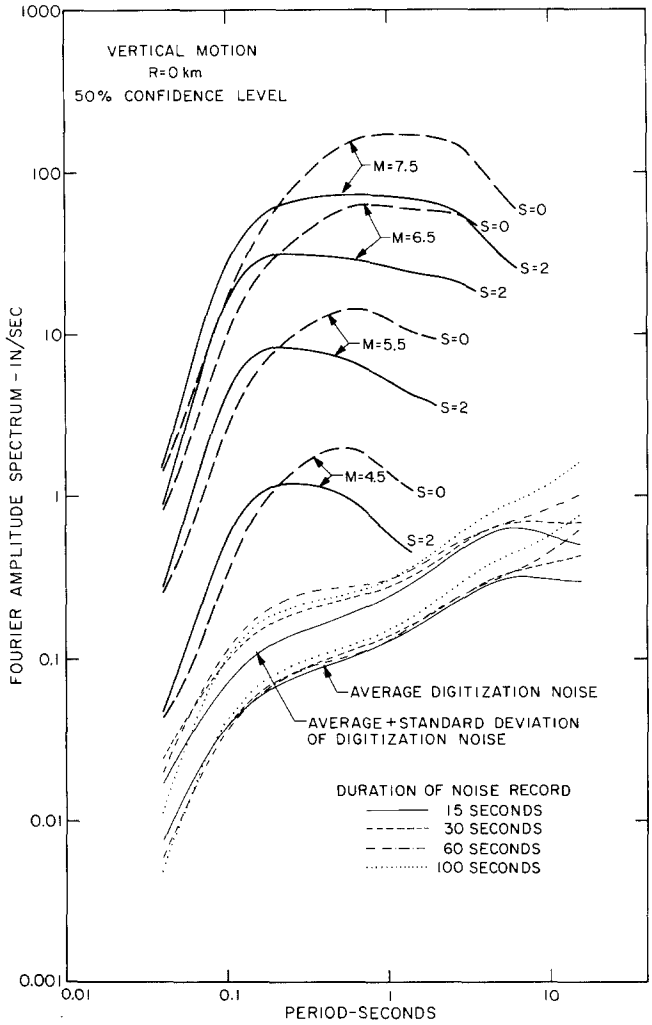

FIG. 4. Vertical Fourier amplitude spectra of strong-motion acceleration for $R=0$, $p=0.50$, $s=0$ and 2 and for magnitudes equal to 4.5, 5.5, 6.5, and 7.5.

noise does not include all possible sources of long-period errors which have no doubt contributed to the computed Fourier amplitude spectra (Trifunac *et al.*, 1973b). Furthermore, to maintain as many spectra as possible for all periods which were considered in the regression analysis, we did not eliminate those spectral amplitudes that were characterized by low signal-to-noise ratio. The consequence of this has been that the functions $b(T)$, $c(T)$, and $f(T)$ still reflect considerable noise content in the raw data for periods longer than several seconds for magnitudes close to 4.5 and for periods longer than 6 to 8 sec for magnitudes close to 7.5. Thus, the spectra that would be obtained from

equation (2) are not accurate for the periods and magnitudes greater than those just indicated. This limitation is also reflected in Figures 3 and 4 where we terminated the spectra in this long-period range. The long-period cut-off points in those figures have been selected at periods where spectra computed from equation (2) begin to deviate appreciably from the slope equal to -1 and start to approach a constant level. An example of an onset of such deviation can still be seen for the spectra corresponding to $M=6.5$ and 7.5 in Figure 3.

If we assume then that in the immediate near-field, shortly after the fault ceases to move, the particle displacement reaches its static permanent displacement and that no long-period wave energy can be reflected back toward the source, then the spectra in Figures 3 and 4 could be extended by straight lines which are defined by $u2\pi/T$. Estimates of the permanent static displacement, u, can then be computed from Figures 3 and 4; these estimates are shown in Table 5 for $s=0$ and $s=2$ for magnitudes $M=4.5$ and $M=7.5$. If no significant overshoot of ground displacements takes place at the fault, then these estimates of permanent displacements should be consistent with the estimates of peak displacements for $R=0$ and with the estimates computed from the analysis of peak displacement amplitudes (Trifunac, 1976). Table 5 shows that this is indeed the case for $M=7.5$ but also indicates that there exist systematic differences of 0.4 to 0.6 on the logarithmic scale

TABLE 5

COMPARISON OF THE LOGARITHMS OF PEAK DISPLACEMENTS (IN INCHES) AT $R=0$ FROM TRIFUNAC (1976) WITH THE LOGARITHMS OF MAXIMUM PERMANENT DISPLACEMENTS (IN INCHES) COMPUTED BY EXTRAPOLATING FOURIER AMPLITUDE SPECTRA (FIGURES 3 AND 4) BY A STRAIGHT LINE WITH SLOPE EQUAL TO MINUS ONE

M		Horizontal Motion		Vertical Motion	
		$s=0$	$s=2$	$s=0$	$s=2$
4.5	Trifunac (1976), $p=0.5$	-0.18	-0.59	-0.42	-0.83
	This study	-0.61	-1.09	-1.03	-1.45
7.5	Trifunac (1976), $p=0.5$	1.66	1.25	1.42	1.01
	This study	1.64	1.25	1.39	1.01

(factors 2 to 4 on the linear scale) for $M=4.5$. These differences could be attributed to the long-period noise which is present in twice-integrated accelerograms for small and/or distant recordings. As Figures 3 and 4 show, these differences would be eliminated by adding the contribution of digitization noise to the spectra for $M=4.5$ or by eliminating the contribution of noise to the computed peak displacements (Trifunac, 1976).

Further corrections and improvements of the functions $a(T)$, $c(T)$, and $f(T)$ so that they do not depend on contributions from processing and digitization noise, as well as the elimination of considerable noise content in the computed peak displacement (Trifunac, 1976), are, of course, all possible. These corrections would require optimum band-pass filtering to be applied in a different manner for each of the 546 accelerograms used in this study and could be designed in such a way that only selected frequency bands remain so that all data have better than some predetermined signal-to-noise ratio. However, we did not carry out such correction procedures in this paper because many data points would have been eliminated from an analysis that already has only a marginal number of representative accelerograms. Furthermore, such correction procedures would require separate extensive and costly analysis of each accelerogram and would only contribute to better accuracy of $b(T)$, $c(T)$, and $f(T)$ in the frequency range where the overall trends of

spectral amplitudes may be inferred from other theoretical and/or observational analyses. For these reasons, it was decided to postpone this noise elimination scheme for a later time when more strong-motion accelerograms become available.

In the short-period range for small magnitudes (Figures 3 and 4) the signal-to-noise ratio also becomes small. However, because the strong-motion data for all recordings employed in this paper are proportional to acceleration, the noise and the recorded spectra tend to be roughly parallel in the high-frequency range so that poor signal accuracy can be expected only for small and/or distant earthquakes and for very high frequencies. Therefore, the high-frequency noise contributions to digitized accelerograms are typically easier to handle and represent less of a problem than the long-period noise.

The slope of the high-frequency spectra for frequencies between about 10 and 25 Hz (Figures 3 and 4) is close to 3 on the log-log scale. This means that for periods between about 0.04 and 0.1 sec, Fourier spectra behave like T^3. The overall shape of the Fourier amplitude spectra in Figures 3 and 4 could be characterized and enveloped by three straight lines. The first line would have a positive slope of about 3, the second line would have zero slope, while the third line would have slope equal to -1. These lines would be tangent to the high-, intermediate-, and low-frequency portions of spectral amplitudes. The intersection of the first and the second straight lines would characterize the low-period corner frequency (about 6 Hz for horizontal and 7 to 8 Hz for vertical spectra corresponding to $s=2$) where the transition of the slope of about 3 to zero slope takes place. As can be seen from Figures 3 and 4 for $s=2$, this corner does not vary much in the magnitude range from 4.5 to 7.5. The long-period corner frequency, which corresponds to the intersection of two straight lines with zero and -1 slopes, decreases with increasing magnitude. For spectra corresponding to a 50 per cent confidence level and $s=2$, this frequency decreases from about 2 Hz for $M=4.5$ to about 0.5 Hz for $M=7.5$.

The changes of average spectral shapes in Figures 3 and 4 illustrate why one may expect to find that the local magnitude M_L would cease to grow as rapidly as the surface-wave magnitude M_S for magnitudes greater than about 6. M_S is determined from amplitudes of distant 20-sec surface waves. The local magnitude M_L predominantly samples displacement waves centered around 1 Hz. As Figures 3 and 4 show, this means that for magnitudes less than about 6, M_L samples mainly that portion of acceleration Fourier spectra for which the periods are longer than the long-period corner frequency, i.e., it samples the amplitudes where spectra behave like $2\pi u/T$. For magnitudes greater than about 6, the corner periods become longer than 1 sec (Figures 3 and 4) and the amplitude of the Wood-Anderson Seismometer becomes more dependent on the amplitudes of the central band of the Fourier spectra between the two corner frequencies where average acceleration spectra tend to be constant with respect to T and cease to grow appreciably for $M>7.5$.

Figures 5 and 6 illustrate the amplitude and shape-dependence of average ($p=0.5$) Fourier amplitude spectra for $M=6.5$ versus epicentral distance. As it can be seen from equations (2) and (3), the terms $\log_{10} A_0(R)$ and $g(T)R$ govern these distance changes. The term $\log_{10} A_0(R)$ leads to overall amplitude variations which are frequency-independent, while the term $g(T)R$ depends on frequency through $g(T)$ and is linear in R. Since $g(T)$ is negative for all frequencies ($f=1/T$), $g(T)R$ acts to increase $FS(T)$ amplitudes with distance. Because, on the whole, the absolute value of $g(T)$ is smaller for high frequencies and larger for low frequencies, the net effect of $g(T)R$ is to attenuate the high-frequency waves somewhat faster than the low-frequency waves. For 0.04- and 10-sec period waves at epicentral distance $R=200$ km, this relative difference would be about 0.2 on the logarithmic amplitude scale. This is a small difference compared to what might be expected on the basis of frequency-dependent attenuation studies which employ

$\exp(-\pi R/TQ\beta)$, for example. However, if it is remembered that the amplitudes of the long-period near-field motions can have geometric decay as rapid as $1/r^4$ (Haskell, 1969) and that these terms most probably have contributed to the recorded strong ground motions for smaller epicentral distances, then the small differences in attenuation of high- and low-frequency spectral amplitudes become more plausible. This could mean then that the rapid geometric decay of long-period waves with distance, $\sim 1/r^n$ may be comparable to the anelastic decay of high-frequency waves, $\exp(-\pi R/TQ\beta)$, so that the net effect is that the average shape of the Fourier amplitude spectra of strong-motion acceleration is not very sensitive to changes of distance, at least for distances between about 20 and 250 km which are representative of the data studied in this paper.

Figures 5 and 6 show that for $M=6.5$ and distances greater than about 70 to 80 km for horizontal motion and about 50 km for vertical motion, high- and low-frequency Fourier amplitude spectra become comparable to the spectra of digitization noise. While some useful data may still be present in the narrow frequency band close to 0.2-sec period and as far as 200 km away from the source for $M=6.5$ earthquakes, these figures clearly show that for typical instrumentation (Trifunac and Hudson, 1970) little or no useful information may be contained in the strong-motion records which have been obtained at epicentral distances greater than about 200 km. For smaller earthquakes (smaller M) this distance range is, of course, smaller. For conventional accelerographs (Trifunac and Hudson, 1970), as Figures 3 and 4 show, the smallest earthquakes that may be expected to provide some useful information in the limited frequency band between say 0.1 and 1 Hz for epicentral distances less than 10 km would have to have magnitude not less than about 3.5 to 4.0 (e.g., Trifunac and Brune, 1970; Dielman *et al.*, 1975; Trifunac, 1972a, 1972b).

Figures 7 and 8 show an example of how horizontal and vertical spectra computed from equations (2) and (4) compare with the acceleration spectra for the three components of strong-motion recorded at the Pacoima Dam site during the San Fernando, California, earthquake of February 9, 1971. In these figures $\log_{10}\{FS(T)_p\}$ spectra were computed for $p=0.1$, 0.5 and 0.9 so that the interval between the spectra for $p=0.1$ and $p=0.9$ represents an estimate of the 80 per cent confidence interval. As may be seen from these figures, the agreement between the recorded and empirically predicted spectra in this case is very good. The spectra for $p=0.1$ and $p=0.9$ do not only envelope the spectra of recorded accelerograms but also follow the overall amplitude and shape trends quite well. This type of agreement between empirically predicted and actually recorded spectra, however, is probably better than what might be expected in an average case.

An example of worse than average fit is illustrated in Figures 9 and 10 for the spectra of strong-motion accelerograms recorded in El Centro during the Imperial Valley, California, earthquake of 1940. During this earthquake the fault rupture was initiated most probably at a distance of about 10 km, or less, southeast of El Centro. It has been suggested that the faulting then progressed southeast in a sequence of some four separate shocks over a fault length of about 40 km during a time interval of some 25 sec (Trifunac and Brune, 1970; Trifunac, 1972b). The largest of these four events most probably took place toward the southeastern end of the fault, 30 to 40 km away from El Centro. Figures 9 and 10 show that if one approximates this complex sequence by a single earthquake of $M=6.4$ at an epicentral distance of 15 km, the average ($p=0.50$) empirical spectra computed from equation (2) underestimate the spectra of recorded motions in the high-frequency range and overestimate the long-period spectral amplitudes. Although an 80 per cent confidence interval still contains most of the recorded spectral amplitudes, the quality of the fit is poor when compared with the results in Figures 7 and 8. The observed differences can be explained, however, by the complexity of the earthquake source and represent a good example of why the function $a(T)$ has such large amplitudes.

The first event during the Imperial Valley sequence of 1940 (Trifunac, 1972b) most probably took place at an epicentral distance equal to 7 to 15 km, had magnitude $M \approx 5.8$, and was characterized by a large stress drop. These factors could explain larger high-frequency and smaller low-frequency spectral amplitudes in the recorded motions. The largest event in the sequence ($M = 6.2$ to 6.4) probably occurred some 30 to 40 km southeast, and, thus, its contribution to empirically computed long-period spectra would also be smaller than as indicated in Figures 9 and 10 because the large epicentral distance

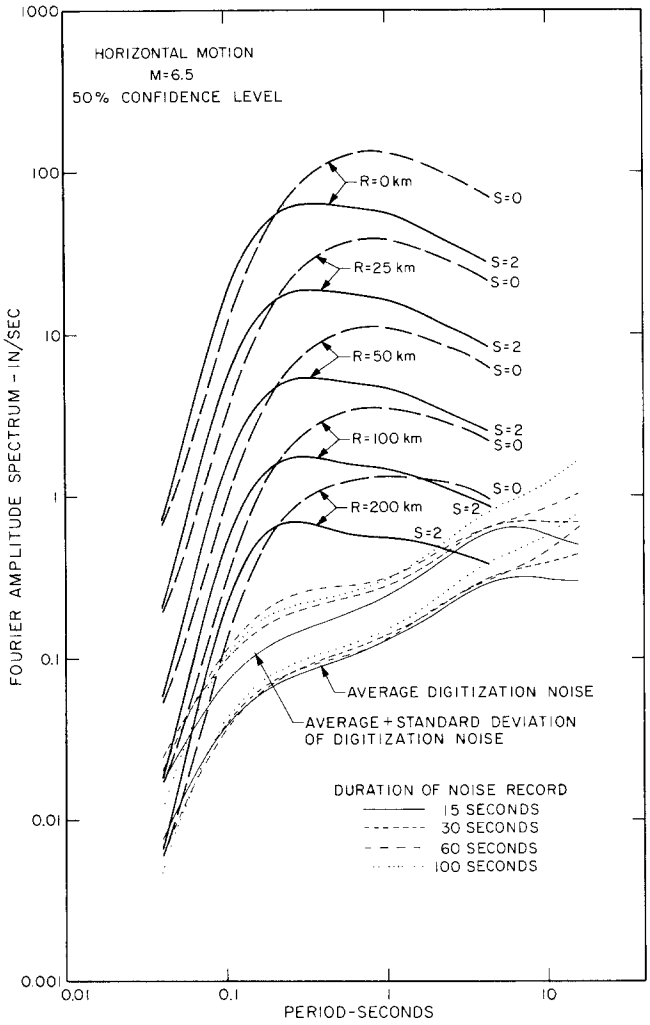

FIG. 5. Horizontal Fourier amplitude spectra of strong-motion acceleration for $p = 0.5$, $s = 0$ and 2, $M = 6.5$, and epicentral distances equal to 0, 25, 50, 100 and 200 km.

would bring the long-period spectral amplitudes further down. Finally, the overall effect of dislocation propagation to the southeast, i.e., away from the recording station, would tend to diminish the long-period waves.

The differences between computed and observed Fourier spectra in Figures 9 and 10 clearly show that the scaling of spectral characteristics of strong earthquake ground motion in terms of earthquake magnitude alone cannot be expected to yield satisfactory answers in all cases, especially for complex earthquake mechanisms. Introduction of

additional parameters into the empirical scaling functions, similar to those which have been presented in equation (2), could be expected to reduce the observed differences. These additional parameters could specify the relative source-to-station geometrical position more precisely than is now done by epicentral distance alone and could describe such properties of the earthquake sources as radiation pattern and the direction and velocity of the propagating dislocation. The compilation of these additional parameters could be carried out during detailed source mechanism studies. Such studies have now been carried

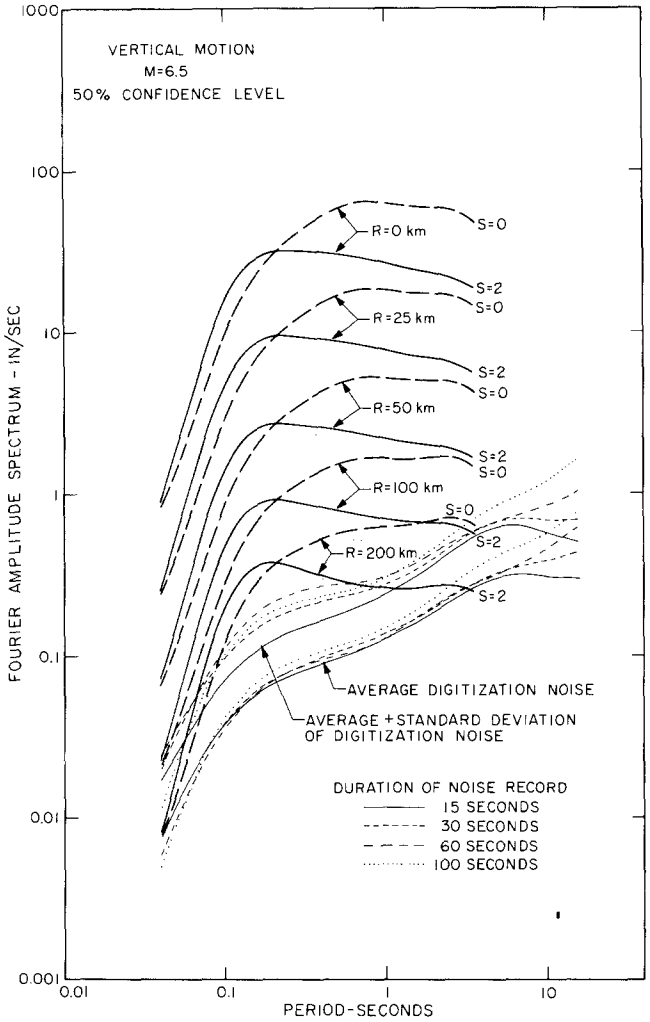

FIG. 6. Vertical Fourier amplitude spectra of strong-motion acceleration for $p=0.5$, $s=0$ and 2, $M=6.5$, and epicentral distances equal to 0, 25, 50, 100 and 200 km.

out for several earthquakes that lead to the data base which is used in this paper (e.g., Trifunac and Brune, 1970; Trifunac, 1972b; Trifunac, 1972a; Trifunac, 1974; Trifunac and Udwadia, 1974). While such *a posteriori* refinements of the empirical models will, no doubt, become possible when more data become available for well-documented and carefully studied earthquakes, the practical question still remains: How feasible will it be to obtain detailed characterization of possible future earthquakes *a priori*? Detailed investigations may enable one to estimate the possible location and probable size (e.g., magnitude and/or fault length) of a future earthquake; if this earthquake is predicted to

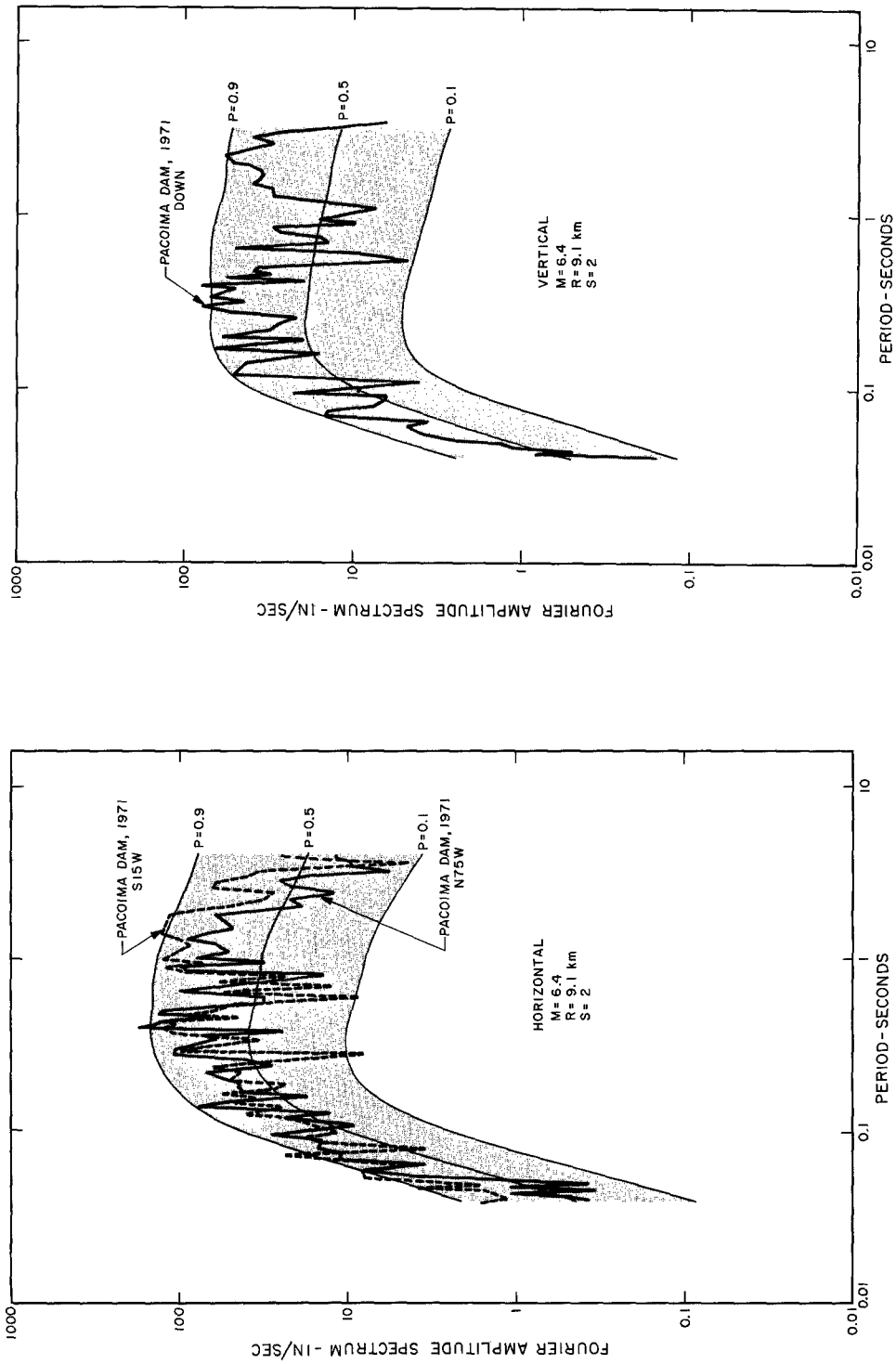

FIGS. 7 AND 8. Comparison of spectra computed from recorded accelerograms with an estimate derived from empirical method.

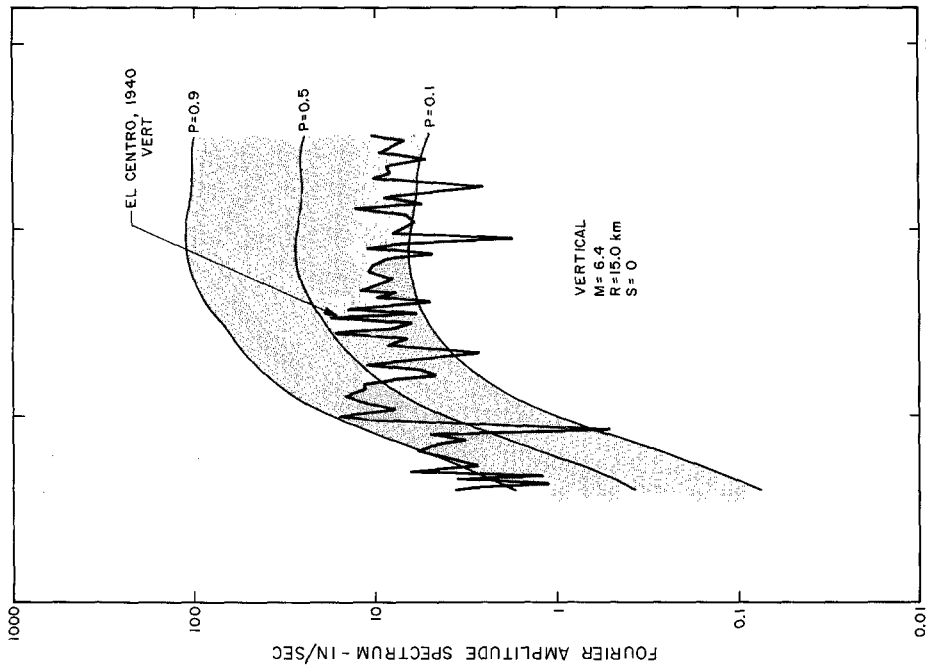

FIG. 10.

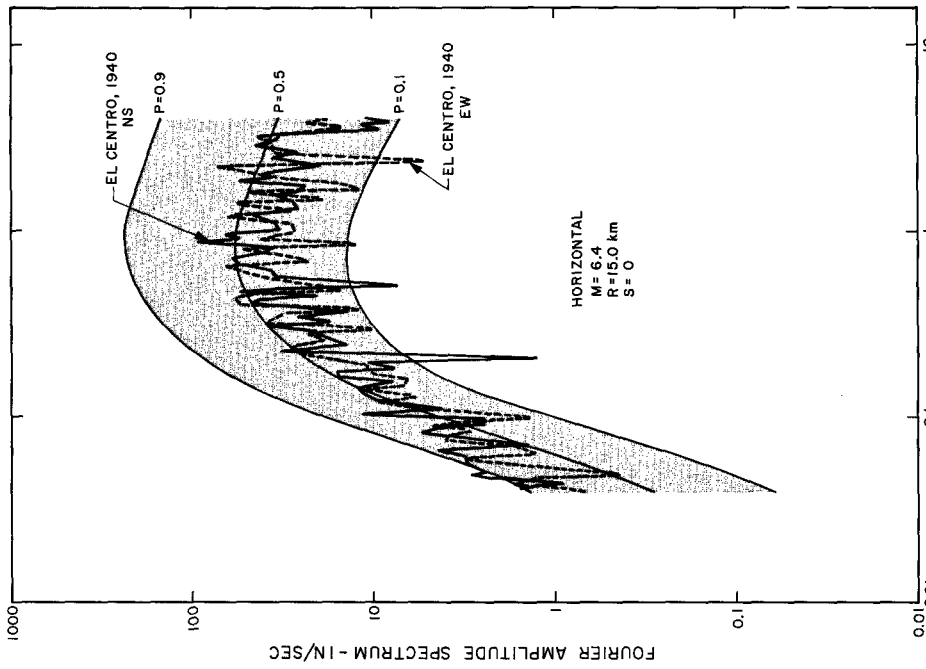

FIG. 9.

FIGS. 9 AND 10. Comparison of spectra computed from recorded accelerograms with an estimate derived from empirical model.

occur on the existing fault, the relative position of the fault to the station may also be known. However, such details as the stress-drop, the direction and the velocity with which dislocation will propagate, and the possible multiplicity of the source appear to be quite difficult to predict at this time. Therefore, for practical earthquake engineering applications, it may be desirable to work with empirical scaling functions which are purposely not more detailed than equation (2), for example, so that the empirical models themselves do not imply smaller uncertainties than those which have to be associated with the input parameters.

Limitations of this Analysis and Possibilities for Future Improvements

There are several important limitations of this study which are related to the number and the type of data which were available for the analysis. First, the total of 182 records, 546 accelerograms, seem to be only barely sufficient to indicate approximate and overall amplitudes of the assumed model for Fourier amplitude spectra. At the present rate of gathering data, it will take many more instrument years before a tenfold or so increase in the total number of records can be expected to become available. The present data and this analysis suggest that at least 2000 records may be required to enable the development of the next generation of better and more detailed theoretical models for scaling the Fourier amplitude spectra of strong ground motion. The presently available 182 records are unevenly distributed among different magnitude levels, and most of them have been recorded at stations located on alluvium. Finally, more than one half of the 182 records were obtained during the San Fernando earthquake of 1971. Since this earthquake does not necessarily represent a typical shock in southern California, this may have introduced a systematic bias into some of the results of this paper.

The function $\log_{10} A_0(R)$ has been assumed to describe the spectral amplitude variations with distance. This function represents an average trend of observed variations of peak amplitudes recorded on a Wood-Anderson seismometer in southern California (Richter, 1958). The advantage in using this function is that it contains information on the average properties of wave propagation through the crust in California where virtually all strong-motion data have been recorded. The disadvantages and limitations, however, which result from using $\log_{10} A_0(R)$ in equation (2) are that its shape does not depend on magnitude, i.e., source dimension of an earthquake, on the geological environment ($s = 0, 1$ and 2) of the recording station, or on the actual amplitudes of recorded motions. That $\log_{10} A_0(R)$ or its analog should depend on the geometric size of the fault has been discussed in some detail, for example, by Dietrich (1973) and need not be repeated here. These magnitude dependent changes of $\log_{10} A_0(R)$ would be such that for small R the slope of $\log_{10} A_0(R)$ would tend to be steeper for earthquakes with small fault dimensions, while for large faults and for small R, $\log_{10} A_0(R)$ would tend to flatten out and have a smaller slope than the average function we employ in this paper. To detect these changes of shape it would be necessary to have many near-field records for different magnitude ranges. Since only very few of the 182 records have been obtained at epicentral distances less than about 10 km, the empirical derivation of different shapes of $\log_{10} A_0(R)$, or its equivalent, for different magnitudes or source dimensions does not seem to be feasible at this time. The shape of the $\log_{10} A_0(R)$ curve may also be expected to depend on deviations from the average properties of the propagation path in California and the geological environment of the recording station. Finally, the amplitudes of waves may be distorted in the near-field and for large amplitudes by the nonlinear response of shallow and surface-soil deposits beneath and surrounding the recording station.

The functional form of the proposed correlation function, equation (2), seems to

represent an adequate approximation for empirical modeling in terms of earthquake magnitude, M, and epicentral distance, R, provided $A_0(R)$ and $FS_0(T, M, p, s, v, R)$ can be chosen to satisfy the trends indicated by the recorded accelerograms. As we indicated in the above discussion, if one assumes that $A_0(R)$ can be approximated by the empirical $A_0(R)$ function (Richter, 1958), which has been proposed for scaling local earthquake magnitude scale, then it becomes possible to determine the coefficients in the assumed empirical model for $FS_0(T, M, p, s, v, R)$. The functional forms for $FS_0(T, M, p, s, v, R)$ which could be based on the fundamental physical principles that govern strong ground motion and reflect the characteristics of the instrumentation used to record this motion are not fully known at this time and would be complicated and possibly too detailed for simple empirical scaling that may be useful in routine applications. For this reason, we considered an approximate representation of $FS_0(T, M, p, s, v, R)$ (equation, 3)

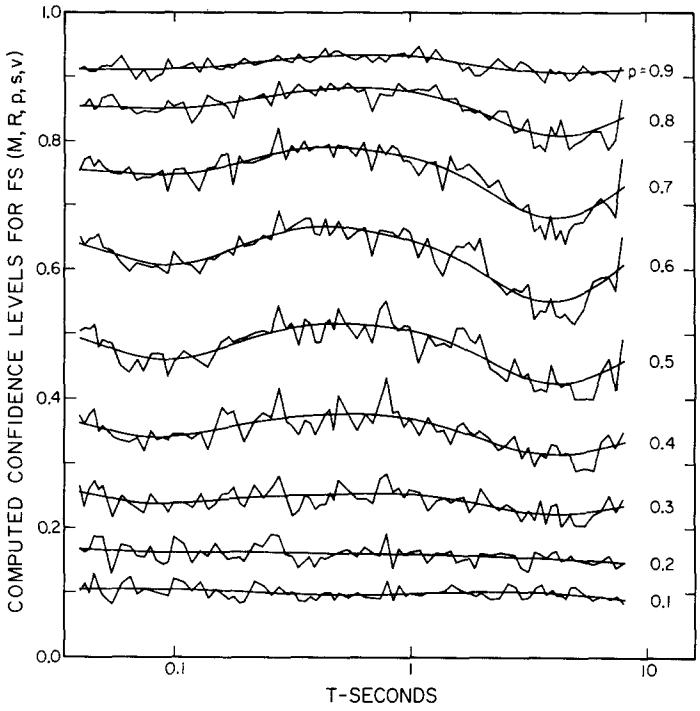

FIG. 11. Actual confidence levels corresponding to the assumed confidence levels p in the linear distribution model.

which is convenient for linear regression analysis and at the same time reflects the simplicity and limitations which are imposed on this analysis. This expression $[\log_{10}\{FS_0(T, M, p, s, v, R)\}]$ is linear in p, s, and v, has linear $[g(T)R]$ dependence on R, and is quadratic in M in the interval $M_{\min} \leqq M \leqq M_{\max}$, linear for $M \geqq M_{\max}$, and constant for $M \leqq M_{\min}$. Higher-order terms in equation (3) and the cross product terms which would contain all or some combination of p, s, v and M have been omitted from the analysis to avoid possibly biased inferences which might result from nonuniform distribution of available data points over the required intervals of p, s, M and R.

The assumed nonlinear nature of $\log_{10} FS_0(T, M, p, s, v, R)$ versus M in $M_{\min} \leqq M \leqq M_{\max}$ has been inferred from several previous investigations which were based on the same set of strong-motion records (Trifunac and Brady, 1975b; Trifunac and Brady, 1976; Trifunac, 1976). However, the parabolic dependence on M represents only a rough approximation to a function which is as yet not known.

In equation (3) we assumed linear dependence on p to permit linear regression analysis and because the actual distribution of spectral amplitudes about the mean level is not known *a priori*. Once the estimates for $a(T), b(T), \ldots, f(T)$ and $g(T)$ are known for a given T, it becomes possible to calculate the fraction of points which lie below and above the predicted amplitudes of $FS(T)_p$ for a given value of p and for the known M, R, S and v corresponding to each recorded spectrum. This computation has been carried out for all periods, for $p=0.1, 0.2, \ldots, 0.8$ and 0.9 and for all Fourier spectra of 546 accelerograms which were used in this study. The result of this calculation, which yields actual confidence levels with respect to the model in equation (2) for the selected $p=0.1, 0.2, \ldots, 0.8$ and 0.9 in the linear term, $a(T)p$, in equation (3), is shown in Figure 11. The smoothed confidence levels for the nine values of p are also shown in this figure. Therefore, if calculation of $FS(T)_p$ is required for actual confidence levels with respect to the assumed model in equation (2), one can find by simple interpolation the correct p value to be used in the linearized model in equation (3) from Figure 11. It should be emphasized, however, that Figure 11 does not show the actual distribution of Fourier spectrum amplitudes, but rather the distribution relative to the assumed approximate representation of spectra in terms of equations (2) and (3).

Conclusions

In this paper a new method for empirical scaling of Fourier amplitude spectra of strong earthquake ground motion has been presented. The functional form of this correlation model has been chosen to reflect the known physical principles that govern the earthquake energy release at the source, the transmission path and the recording conditions. Although an effort has been made to derive the representative scaling functions for this model by using all the digitized and corrected data which are available in the United States so far, it should be emphasized here that the detailed characteristics of the model and the smoothed numerical values of its scaling functions $a(T), b(T), \ldots, g(T)$ represent only preliminary and approximate estimates which will have to be improved when more recordings become available. Therefore, the results presented in this paper can only be taken as suggestive of actual overall trends that characterize the Fourier amplitude spectra of strong earthquake ground motion. Some inferences, although seemingly real, may only reflect the weaknesses of the model and/or the inadequate and incomplete set of data which we used to estimate them. In spite of these limitations, however, the only sound approach toward a complete solution of this problem is to examine the simple and obvious trends which can be extracted from actual recordings and to use these trends on an interim basis as a vehicle for the development of better recording and analyzing techniques in the future.

On the logarithmic scale the Fourier amplitude spectra of strong-motion accelerations tend to increase linearly with magnitude for shocks which are typically less than $M=4.0$ to $M=5.5$. For larger magnitudes the rate of growth of spectral amplitudes slows down and the amplitudes seem to reach maxima for the magnitude range between $M=7.5$ and $M=8.5$. The shape of the average Fourier amplitude spectra changes with magnitude reflecting relatively greater content of long-period waves for larger earthquakes.

For $M=6.5$ earthquakes, at distances close to and greater than 100 km, the Fourier spectra of digitization and processing noise begin to interfere with and become comparable to spectral amplitudes of strong motion. For shocks with magnitude less than $M=4.5$ only a limited frequency band from about 10 to about 1 Hz may be extracted from the records at small epicentral distances which are typically less than 10 km.

The average high-frequency Fourier amplitude spectra for periods shorter than about 0.2 sec appear to be larger for accelerograms which were recorded on basement rock sites

($s=2$) than for the stations that recorded on alluvium ($s=0$) by a factor which is less than about 0.2 on the logarithmic scale. For periods longer than about 0.7 to 0.8 sec this trend is reversed and the average Fourier spectrum recorded on alluvium ($s=0$) is larger by about 0.4 on the logarithmic scale than the spectrum amplitudes of accelerograms recorded on basement rocks ($s=2$).

Vertical components of strong-motion accelerograms lead to Fourier amplitudes which are larger than the horizontal components by a factor less than 0.1 on the logarithmic scale for frequencies higher than 10 Hz. This trend is reversed for periods longer than 0.1 sec. For periods between about 0.3 and 2 sec, horizontal spectra are larger by a factor of about 0.3 on the logarithmic scale. For periods longer than 2 sec this factor decreases from 0.3 to about 0.1 for long periods close to 10 sec.

The changes of shape of the Fourier amplitude spectra with distance have been found to be small and are such that the high-frequency waves are attenuated faster than the long-period waves. For distances less than 50 to 100 km, relative attenuation of the logarithm of Fourier amplitudes can be approximated by $\log_{10}A_0(R)+R/1000$.

The nature of the dependence of the empirical Fourier spectral amplitudes on magnitude and distance could be related to and does not seem to be contradicted by our present understanding of the earthquake source mechanisms. The significance and the extent of the above described changes of spectral shapes, however, cannot be evaluated without a detailed consideration of the uncertainties and the scatter of actual observations relative to the average trends which result from the empirical model. The upper and lower boundaries of the 80 per cent confidence interval, for example, differ by factors equal to 1.1 to 1.4 on the logarithmic scale. This corresponds to factors of about 12 to 25 on the linear amplitude scale and, when compared with the amplitude variations affected by different magnitudes or site conditions, clearly shows that many other features of the actual Fourier amplitude spectra have been omitted in this approximate analysis. These large variations thus illustrate the degree of variability that exists between earthquakes which have been labeled by an identical set of M, R, and s parameters or in other words show the uncertainties that result from the simplistic characterization of strong ground shaking in terms of magnitude, M, epicentral distance, R, and the recording site conditions only. Future improvements may reduce these uncertainties somewhat by introducing more complete and more detailed empirical scaling functions for Fourier amplitude spectra, but it seems likely that the large scatter similar to that which is now described by the $a(T)$ function may remain. If this expectation is correct, it will mean that there is considerable variability in the characteristics of strong ground motion which is caused by complexities at the source and along the wave propagation path, and that this variability cannot be overlooked in the analysis of the trends and amplitude variations which depend on magnitude, distance and site conditions only. This variability will impose a limit on the resolution of source mechanism studies which use the data derived from strong-motion instruments. For practical applications in earthquake engineering and strong-motion seismology, better understanding of these uncertainties will enable one to evaluate the meaning and the adequacy of the computational methods and quantitative and judgmental engineering decisions.

Acknowledgments

I thank J. G. Anderson, J. E. Luco and H. L. Wong for critical reading of the manuscript and several useful suggestions. I am indebted to A. Abdel-Ghaffar, A. G. Brady, B. E. Turner, F. E. Udwadia, B. D. Westermo and H. L. Wong for contributing their time to digitize the sloping straight line used in the analysis of digitization noise.

This research was supported in part by contracts from the U.S. Geological Survey and Nuclear Regulatory Commission and by the Earthquake Research Affiliates Program of the California Institute of Technology.

REFERENCES

Brune, J. N. (1970). Tectonic Stress and the spectra of seismic shear waves from earthquakes, *J. Geophys. Res.* **75,** 4997–5009.

Dielman, R. J., T. C. Hanks, and M. D. Trifunac (1975). An array of strong-motion accelerographs in Bear Valley, California, *Bull. Seism. Soc. Am.* **65,** 1–12.

Dietrich, J. H. (1973). A deterministic near-field source model, *Proc. World Conf. Earthquake Eng., 5th, Rome,* Italy.

Gutenberg, B. (1957), Effects of ground on earthquake motion, *Bull. Seism. Soc. Am.* **47,** 221–250.

Gutenberg, B. and C. F. Richter (1956). Earthquake magnitude, intensity, energy and acceleration, Paper II, *Bull. Seism. Soc. Am.* **46,** 105–195.

Hanks, T. C. and M. Wyss (1972). The use of body-wave spectra in the determination of seismic source parameters, *Bull. Seism. Soc. Am.* **62,** 561–590.

Haskell, N. A. (1969). Elastic displacements in the near-field of a propagating fault, *Bull. Seism. Soc. Am.* **59,** 865–908.

Hudson, D. E., A. G. Brady, and M. D. Trifunac (1972a). Strong Motion Accelerograms, Response Spectra, Volume III, Part A, *EERL 72–80,* Earthquake Eng. Res. Lab., Calif. Inst. of Tech., Pasadena.

Hudson, D. E., A. G. Brady, M. D. Trifunac, F. E. Udwadia, and A. Vijayaraghavan (1972b). Strong-Motion Earthquake Accelerograms, Fourier Spectra, Volume IV, Part A, *EERL 72–100,* Earthquake Eng. Res. Lab., Calif. Inst. of Tech., Pasadena.

Hudson, D. E., A. G. Brady, M. D. Trifunac, and A. Vijayaraghavan (1971). Strong-Motion Earthquake Accelerograms, Corrected Accelerograms and Integrated Ground Velocity and Displacement Curves, Volume II, Part A, *EERL 71–50,* Earthquake Eng. Res. Lab., Calif. Inst. of Tech., Pasadena.

Mikumo, T. (1973). Faulting process of the San Fernando earthquake of February 9, 1971 inferred from static and dynamic near-field displacements, *Bull. Seism. Soc. Am.* **63,** 249–264.

Richter, C. F. (1958). *Elementary Seismology,* Freeman, San Francisco.

Savage, J. C. (1966). Radiation From a Realistic Model of Faulting, *Bull. Seism. Soc. Am.* **56,** 577–592.

Thatcher, W. and T. C. Hanks (1973). Source Parameters of Southern California Earthquakes, *J. Geophy. Res.* **78,** 8547–8576.

Trifunac, M. D. (1972a). Stress estimates for San Fernando, California, earthquake of February 9, 1971: Main event and thirteen aftershocks, *Bull. Seism. Soc. Am.* **62,** 721–750.

Trifunac, M. D. (1972b). Tectonic stress and source mechanism of the Imperial Valley, California, earthquake of 1940, *Bull. Seism. Soc. Am.* **62,** 1283–1302.

Trifunac, M. D. (1973). Analysis of strong earthquake ground motion for prediction of response spectra, *Intern. J. Earthquake Eng. Struct. Dynamics,* **2,** 59–69.

Trifunac, M. D. (1974). A three-dimensional dislocation model for the San Fernando, California, earthquake of February 9, 1971, *Bull. Seism. Soc. Am.* **64,** 149–172.

Trifunac, M. D. (1976). Preliminary analysis of the peaks of strong earthquake ground motion—Dependence of peaks on earthquake magnitude, epicentral distance and the recording site conditions, *Bull. Seism. Soc. Am.* **66,** 189–219.

Trifunac, M. D. and A. G. Brady (1975a). On the correlation of seismic intensity scales with the peaks of recorded strong ground motion, *Bull. Seism. Soc. Am.* **65,** 139–162.

Trifunac, M. D. and A. G. Brady (1975b). On the correlation of peak accelerations of strong motion with earthquake magnitude, epicentral distance and site conditions, *Proc. U.S. Natl. Conf. Earthquake Eng., Ann Arbor,* Michigan, 43–52.

Trifunac, M. D. and A. G. Brady (1976). Correlations of peak acceleration, velocity and displacement with earthquake magnitude, distance and site conditions, *Intern. J. Earthquake Eng.* and *Struct. Dynamics* (in press).

Trifunac, M. D., A. G. Brady, D. E. Hudson, and T. C. Hanks (1973b). Strong-Motion Earthquake Accelerograms, Volume II, Part G, *EERL 73–52,* Earthquake Eng. Res. Lab., Calif. Inst. of Tech., Pasadena.

Trifunac, M. D. and J. N. Brune (1970). Complexity and energy release during the Imperial Valley, California, earthquake of 1940, *Bull. Seism. Soc. Am.* **60,** 137–160.

Trifunac, M. D. and D. E. Hudson (1970). Laboratory evaluation and instrument corrections of strong-motion accelerographs, *EERL70–04,* Earthquake Eng. Res. Lab., Calif. Inst. of Tech., Pasadena.

Trifunac, M. D. and V. W. Lee (1973). Routine computer processing of strong-motion accelerograms, *EERL73–03,* Earthquake Eng. Res. Lab., Calif. Inst. of Tech., Pasadena.

Trifunac, M. D. and V. W. Lee (1974). A note on the accuracy of computed ground displacements from strong-motion accelerograms, *Bull. Seism. Soc. Am.* **64,** 1209–1219.

Trifunac, M. D. and F. E. Udwadia (1974). Parkfield, California, earthquake of June 27, 1966: A three-dimensional moving dislocation, *Bull. Seism. Soc. Am.* **64,** 511–533.

Trifunac, M. D., F. E. Udwadia, and A. G. Brady (1973a). Analysis of errors in digitized strong-motion accelerograms, *Bull. Seism. Soc. Am.* **63,** 157–187.

Tucker, B. E. (1975). Source Mechanisms of Aftershocks of the 1971 San Fernando, California Earthquake, *Ph.D. Thesis*, U. California, San Diego.

Udwadia, F. E. and M. D. Trifunac (1974). Characterization of response spectra through the statistics of oscillator response, *Bull. Seism. Soc. Am.* **64,** 205–219.

Udwadia, F. E. and M. D. Trifunac (1975). A Note on the Calculation of Fourier Amplitude Transforms, (Abstract), Presented during the 1975 Annual Meeting of the Seismological Society of America, Cal. State Univ., Los Angeles.

EARTHQUAKE ENGINEERING RESEARCH LABORATORY
MAIL CODE 104–44
CALIFORNIA INSTITUTE OF TECHNOLOGY
PASADENA, CALIFORNIA 91125

Manuscript received December 22, 1975